

THE IMF LONG AGO AND FAR AWAY:

Faint Stars in the Ursa Minor dSph Galaxy

Rosemary F.G. Wyse

Johns Hopkins University

Department of Physics & Astronomy

wyse@pha.jhu.edu

Abstract The dwarf spheroidal galaxy in Ursa Minor is apparently dark-matter dominated, and is of very low surface brightness, with total luminosity only equal to that of a globular cluster. Indeed its dominant stellar population is old and metal-poor, very similar to that of a classical halo globular cluster in the Milky Way Galaxy. However, the environment in which its stars formed was clearly different from that in the globular clusters in the Milky Way Galaxy – what was the stellar IMF in this external galaxy a long time ago? The fossil record of long-lived, low-mass stars contains the luminosity function, derivable from simple star counts. This is presented here. The mass function requires a robust mass-luminosity relation, and we describe the initial results to determine this, from our survey for eclipsing low-mass binaries in old open clusters. The massive star IMF at early times is constrained by elemental abundances in low-mass stars, and we discuss the available data. All data are consistent with an invariant IMF, most probably of Salpeter slope at the massive end, with a turnover at lower masses.

Introduction

The stellar IMF at high redshift is of great importance for a wide range of astrophysical problems, such as the ionization and enrichment of the intergalactic medium, the extragalactic background light, the visibility of galaxies and the rate at which baryons are locked-up into stars and stellar remnants. There are two complementary approaches to the determination of the IMF long ago and far away: one is to observe directly high redshift objects, and attempt inferences on the stellar IMF from the integrated spectrum and photometry, while the second approach analyses the fossil record in old stars at low redshift. The characterization of the stellar IMF in external galaxies, compared to that in the Milky

Way, is a crucial step in deciphering the important physical processes that determine the distribution of stellar masses under a range of different physical conditions. The low mass stellar IMF at the high redshifts at which these stars formed is directly accessible through star counts, plus a mass-luminosity relation. The high mass IMF at these high redshifts is constrained by the chemical signatures in the low mass stars that were enriched by the supernovae from the high mass stars. I will discuss both ends of the IMF at high redshift, in an external galaxy.

1. Extremely Old Stars

Simulations of galaxy formation within the framework of the ‘concordance’ (Λ)CDM cosmology agree that the first stars form within structures that are less massive than a typical L_* galaxy today (e.g. Kauffmann, White & Guiderdoni 1993; Cole et al. 2000). Large galaxies form hierarchically, through the merging and assimilation of such smaller systems. Satellite galaxies of the Milky Way are survivors of this merging (e.g. Bullock, Kravtsov & Weinberg 2000). The stars that formed at early times are found, at the present day, throughout large galaxies, and also in satellite galaxies. Environments with little subsequent star formation are the best places to find and study old stars – the stellar halo of the Milky Way, and a few of the dwarf spheroidal satellite galaxies.

1.1 The Ursa Minor Dwarf Spheroidal Galaxy

The dwarf spheroidal galaxy in Ursa Minor (UMi dSph), like all members of its morphological class (Gallagher & Wyse 1994), has extremely low surface brightness, with a central value of only ~ 25.5 V mag/sq. arcsec, or $\sim 2.5 L_\odot/\text{pc}^{-2}$. The total luminosity is in the range $2 - 4 \times 10^5 L_{V,\odot}$ (Kleyna et al. 1998; Palma et al. 2003), equal to that of a luminous Galactic globular cluster. Again similar to a globular cluster, the Ursa Minor dSph contains little or no gas and has apparently not formed a significant number of stars for ~ 12 Gyr (e.g. Hernandez et al. 2000; Carrera et al. 2002), or since a redshift $z \gtrsim 2$. The metallicity distribution of the stars is narrow, with a mean of $[\text{Fe}/\text{H}] \sim -1.9$ dex and a dispersion of ~ 0.1 dex (e.g. Bellazzini et al. 2002). The stellar line-of-sight velocity dispersion is ~ 10 km/s (e.g. Wilkinson et al. 2004), sufficiently large that, unlike globular clusters, equilibrium models have a large mass-to-light ratio, $(\mathcal{M}/L)_V \gtrsim 50 (\mathcal{M}/L)_{V,\odot}$, perhaps as high as several hundred in solar units if the mass is $\gtrsim 10^8 \mathcal{M}_\odot$ (Wilkinson et al. 2004), indicating a non-baryonic dark halo. Non-equilibrium models are rather contrived and themselves fail to explain the data (e.g. Wilkinson et al. 2004). Models of the evolution of dwarf spheroidals are by no

means well developed, but very likely the stars formed in an environment rather different than that of globular cluster stars, or of current star-forming regions in the disk of the Milky Way.

The distance of the Ursa Minor dSph is only ~ 70 kpc, close enough that a determination of the luminosity function of low-mass main sequence stars through star counts is feasible, particularly using the Hubble Space Telescope. The (unusually) simple stellar population of this dwarf spheroidal – essentially of single age, single metallicity – makes the derivation of the luminosity function from star counts a robust procedure. This determines the low-mass stellar IMF at redshifts of $\gtrsim 2$. High-resolution spectroscopy of the luminous evolved stars is also possible, yielding elemental abundances which constrain the high-mass stellar IMF that enriched the low-mass stars we observe.

2. The Faint Stellar Luminosity Function and Mass Function at Redshift $\gtrsim 2$

The (very) dominant stellar population in the UMi dSph is very similar to that of a classical Galactic halo globular cluster. The most robust constraint on the low-mass stellar IMF is then obtained by a direct comparison between the faint stellar luminosity functions of the UMi dSph and of representative globular clusters of the same age and metallicity, such as M15 and M92, observed in the same bandpasses, same telescope and detector. With the same stellar populations, this is a comparison between *mass* functions, and differences may be ascribed to variations in the low-mass IMF.

We therefore obtained deep images with the Hubble Space Telescope in a field close to the center of the UMi dSph, using STIS as the primary instrument (optical Long Pass filter), with WFPC2 (V_{606} and I_{814} filters) and NICMOS (NIC2/H-band) in parallel. The WFPC2 filters matched those of extant data for M15 and M92; we obtained our own STIS/LP and NIC2/H-band data for M15. Similarly exposed data for an ‘off’ field, at 2–3 tidal radii from the centre of UMi dSph, were also acquired. The detailed paper presenting the results from the full dataset is Wyse et al. (2002); preliminary results from a partial WFPC2 dataset were presented in Feltzing, Wyse & Gilmore (1999).

The images are not crowded and standard photometric techniques were used to derive the luminosity functions. For the WFPC2 data, the luminosity functions were based only upon stars (unresolved objects) that lie close to the well-defined UMi dSph main sequence locus in the colour-magnitude diagram (CMD; see Figure 1). The ‘off’ field CMD confirmed little contamination from Galactic stars. The STIS lu-

minosity function was based on one band only, and we employed various approaches to background subtraction. The NICMOS data served only to exclude a hypothetical population of very red stars and will not be discussed further here. The extant WFPC2 data for the globular clusters (Piotto et al. 1997) are from fields at intermediate radii within the clusters, where effects of dynamical evolution on the mass function should be minimal.

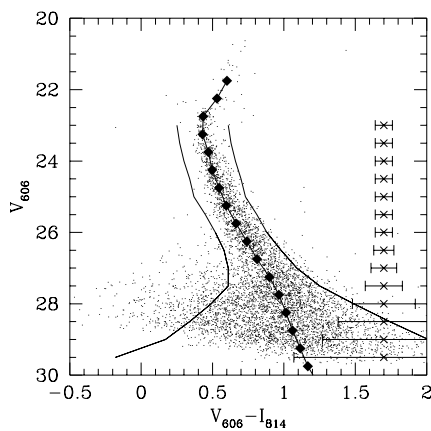


Figure 1
From Wyse et al. (2002). Colour-magnitude diagram for all UMi dSph stars from the three wide-field cameras on WFPC2. The full curves delineate the selection criteria for stars to be included in the luminosity function. The error-bars in each magnitude bin are shown at the right. The well-defined narrow main sequence is the main feature. The few blue stars close to the turn-off are probably blue stragglers, rather than younger stars. The distribution of stars across the main sequence is asymmetric, to the red, and is consistent with a normal population of binary stars.

2.1 Comparisons with Globular Clusters

The comparisons with the WFPC2 colour-magnitude based V-band and I-band luminosity functions are shown in Figure 2. We adopted 0.5 mag bins to have reasonable numbers in each bin, and to minimize effects of e.g. reddening and distance moduli uncertainties. The 50% completeness limits for the UMi dSph data are equivalent to absolute magnitudes of $M_{606} = +9.1$ and $M_{814} = +8.1$, which using the Baraffe et al. (1997) models *both* correspond to masses of $\mathcal{M} \sim 0.3 \mathcal{M}_{\odot}$. The STIS/LP data provide an independent check, by both a direct LP-luminosity function comparison between M15 and UMi dSph, and a derived STIS-based I-band luminosity function. All show that the globular cluster stars and the UMi stars have indistinguishable faint luminosity functions, down to an equivalent mass limit of $\sim 0.3 \mathcal{M}_{\odot}$ (see Wyse et al. 2002 for details).

We employed various statistical tests to quantify the agreement of the various datasets – e.g. STIS-derived I-band *vs.* WFPC2 I-band etc:

♡ Linear, least-square fits to the (log) counts as a function of apparent magnitude, using various ranges of magnitude and differing bin choices, consistently found agreement to better than 2σ .

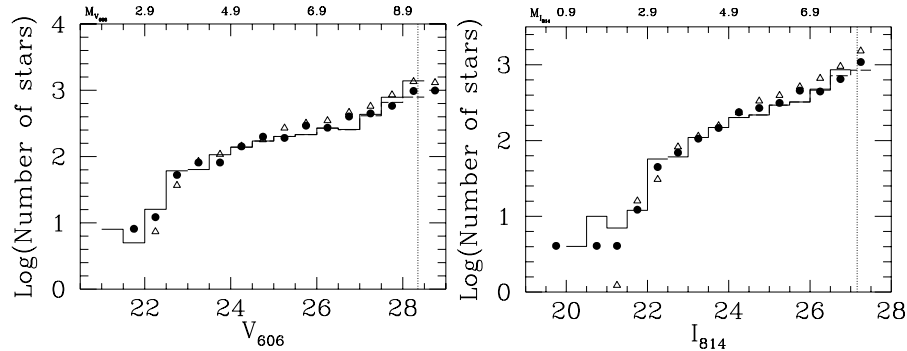


Figure 2. Based on figures in Wyse et al. (2002). Comparisons between the completeness-corrected Ursa Minor luminosity functions (histograms; 50% completeness indicated by the vertical dotted line) in the V-band (left panel) and the I-band (right panel) and the same for M92 (filled circles) and M15 (open triangles) (both taken from Piotto et al. 1997, renormalized and shifted to the same distance as the Ursa Minor dSph). The luminosity functions for the globular clusters and the dwarf spheroidal galaxy are indistinguishable.

♡ Kolmogorov-Smirnov tests on the unbinned data for a variety of magnitude ranges; the results depend on systematics such as the relative distance moduli, but again there is general agreement to better than 5% significance level.

♡ χ -square tests were carried out on the binned data, using a variety of bin centers (maintaining 0.5 mag bin widths) and magnitude ranges and again agreement to better than 5% significance level.

The main result is that the underlying mass functions of low-mass stars in Galactic halo globular clusters and in the external galaxy the UMi dSph are indistinguishable. This is a comparison between two different galaxies, and systems of very different baryonic densities and dark matter content.

3. Low-Mass Stellar Mass Functions

Adopting the Baraffe et al. (1997) models, the 50% completeness limits for the luminosity functions of the stars in the UMi dSph correspond to $\sim 0.3 M_{\odot}$, and the mass function may be fit by a power law, with slope somewhat flatter than the Salpeter (1955) value, over the range we test, of $0.3 \lesssim M/M_{\odot} \lesssim 0.8$. This is consistent with the solar neighbourhood mass function over this mass range, and indeed the universal mass function that appears to be the conclusion of this meeting.

However, the light-to-mass transformation is not robustly defined for K/M dwarfs, especially as a function of age and metallicity. Calibration of this is best achieved by analysis of low-mass stars in detached eclipsing binary systems, and we have recently undertaken a photometric survey

of open clusters to identify candidate low-mass binary systems to be followed up with spectroscopy for radial velocity curves; this forms the PhD thesis of Leslie Hebb at Johns Hopkins University.

Our sample consists of six open clusters of known age and metallicity (from the brighter turn-off stars), old enough to have low-mass stars on the main sequence, age $\gtrsim 2 \times 10^8$ yr, with the oldest being ~ 4 Gyr. We used both the Wide Field Camera on the 2.5m Isaac Newton Telescope and the Mosaic Camera on the Kitt Peak 4m telescope, each of which provide a field of view of $\sim 35' \times 35'$. The observing strategy we adopted was designed to enable the detection of a 0.05 mag amplitude eclipse in a target $0.3 M_{\odot}$ star, monitored on timescales of fraction of an hour, hours and days. The low probability of eclipse means that populous clusters must be observed for many days. We expect our survey to find 3–5 low-mass eclipsing systems. The details of the survey are presented in Hebb, Wyse & Gilmore (2004).

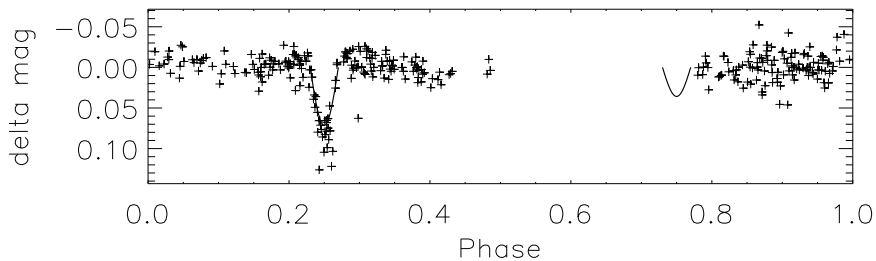


Figure 3. The phase-folded lightcurve for a candidate M-dwarf eclipsing system in the open cluster M35, with a period of just over 1 day. The crosses show all differential photometry measurements for this object collected in January 2002, January 2003 and February 2003. The solid line is a simple sine-wave fit to the measurements taken during the primary eclipse. The phase of the secondary eclipse is marked by the same sine function fit to the primary eclipse, but with half the amplitude.

The imaging data has all been acquired, differential photometry obtained and we are now analyzing the derived light curves. An example of the light curve of a candidate eclipsing low-mass system is shown in Figure 3; the candidate was identified by applying a box-fitting algorithm to the photometric time series. Our photometry, plus infrared data from 2MASS, is consistent with this being an M-dwarf system. We have applied for follow-up spectroscopic data, together with higher time-sampling photometric data, for this system and for our other candidates.

4. High-Mass Stellar Mass Functions

The high-mass stellar mass function long ago can be constrained by the elemental abundances in the long-lived low-mass stars that formed

from gas that was enriched by the Type II supernovae from the massive stars of a previous generation (see e.g. review of Wyse 1998). Interpretation of the pattern of elemental abundances is easiest for low-mass stars that formed early in a star-formation event, and were enriched by *only* massive stars. Most of the dwarf spheroidal companions to the Milky Way have had extended star formation, and so are expected to show evidence in the elemental abundances for the incorporation of iron from long-lived Type Ia supernovae. The Ursa Minor dSph is the best candidate for having had a sufficiently short duration of star formation that a significant fraction of its low-mass stars formed prior to the onset of Type Ia supernovae in sufficient numbers to be noticed in the chemical elemental abundances; this timescale is uncertain, but likely to be of the order of 1–2 Gyr.

The elemental mix produced by a generation of massive stars depends on the massive-star mass function, because the yields of a given Type II supernova depends on its mass. In particular, the α -element yields (nuclei formed by successive addition of a helium nucleus) vary more strongly with progenitor mass than does the iron yield (e.g. Figure 1 of Gibson 1998). There appears to have been surprisingly good mixing at early times, at least in the stellar halo of the Milky Way (see the remarkably low scatter in the ratio of $[\alpha/\text{Fe}]$ at $[\text{Fe}/\text{H}] \lesssim -2.5$ in the sample analysed by Cayrel et al. 2004), so that a well-defined value of $[\alpha/\text{Fe}]$ is produced by a generation of massive stars of given IMF. This is seen as the ‘Type II plateau’ in $[\alpha/\text{Fe}]$ for metal-poor Galactic stars.

The available elemental abundance data for a handful of individual stars in the UMi dSph are consistent with the same value for the Type II plateau as seen in stars of the Milky Way (Shetrone et al. 2001), with some downturn for more metal-rich stars, as expected if there is an age spread of 1–2 Gyr and an age-metallicity relationship. The simplest interpretation is that the high mass IMF was the same in the UMi dSph as in the Galaxy – and that IMF is a power-law with Salpeter (1955) slope.

Most of the stars in the other dwarf spheroidals have low values of $[\alpha/\text{Fe}]$, consistent with a standard – Salpeter – IMF for massive stars and an extended star formation history, as implied by their colour-magnitude diagram (see e.g. Venn et al. 2004).

5. Conclusions

The fossil record in low-mass stars at the present time allows the derivation of the stellar IMF at high redshift. The low-mass luminosity function is accessible through star counts, most robustly in a system

with a simple stellar population. We have found that the low-mass IMF is invariant between globular clusters in the halo of the Milky Way and an external galaxy, the dwarf spheroidal in Ursa Minor. The underlying mass function is apparently the same as that for present-day star formation in the local disk of the Milky Way. The low-mass IMF is remarkably invariant, over a broad range of metallicities, age, star-formation rate, baryonic density, dark matter content – indeed most of the parameters that *a priori* one might have expected to be important in determining the masses of stars. The high-mass IMF is also apparently independent of these parameters. This invariance is particularly surprising if the Jeans mass plays an important role.

Acknowledgments

I thank my colleagues and collaborators Sofia Feltzing, Jay Gallagher, Gerry Gilmore, Leslie Hebb, Mark Houdashelt and Tammy Smecker-Hane for their contributions to the results described here. I would also like to thank the tireless organizers of this stimulating meeting for inviting me.

References

- Baraffe, I., Chabrier, G., Allard, F. & Hauschildt, P. 1997, A&A, 327, 1054
 Bullock, J., Kravtsov, A. & Weinberg, D. 2000, ApJ, 539, 517
 Bellazzini, M., Ferraro, F., Origlia, L., Pancino, E. et al. 2002, AJ, 124, 3222
 Carrera, R., Aparicio, A., Martinez-Delgado, D. & Alonso-Garcia, J. 2002, AJ, 123, 3199
 Cayrel, R. et al. 2004, A&A, 416, 1117
 Cole, S., Lacey, C., Baugh, C. & Frenk, C. 2000, MNRAS, 319, 168
 Feltzing, S., Wyse, R.F.G. & Gilmore, G. 1999, ApJL, 516, 17
 Gallagher, J.S. & Wyse, R.F.G. 1994, PASP, 106, 1225
 Gibson, B. 1998, ApJ, 501, 675
 Hebb, L., Wyse, R.F.G. & Gilmore, G. 2004, AJ, December issue (astro-ph/0409289)
 Hernandez, X., Gilmore, G. & Valls-Gabaud, D. 2000, MNRAS, 317, 831
 Kauffmann, G., White, S.D.M. & Guiderdoni, B. 1993, MNRAS, 264, 201
 Kleyna, J., Geller, M., Kenyon, S., Kurtz, M. & Thorstensen, J. 1998, AJ, 115, 2359
 Palma, C., Majewski, S., et al. 2003, AJ, 125, 1352
 Piotto, G., Cool, A. & King, I. 1997, AJ, 113, 1345
 Salpeter, E.E. 1955, ApJ, 121, 161
 Shetrone, M., Côté, P. & Sargent, W. 2001, ApJ, 548, 592
 Venn, K. et al. 2004, AJ, 128, 1177
 Wilkinson, M., Kleyna, J., Evans, W., Gilmore, G., Irwin, M. & Grebel, E. 2004, ApJL, 611, 21
 Wyse, R.F.G. 1998, in The Stellar IMF, ASP Conf series 142, eds Gilmore & Howell, p89
 Wyse, R.F.G. et al. 2002, New Ast, 7, 395